METHANOGENESIS MECHANISMS AND MICROBIAL ECOLOGY IN THE ANAEROBIC CO-DIGESTION OF SLUDGE AND GREASE
/
污泥-油脂厌氧共消化过程中的产甲烷机制及微生物生态学探究

Chenxi LI[1)], Jinku LIU[1)], Mengjie DU[1)], Chundong WU[*1)], Zhanbin GUO[*1)]
[1)]College of Engineering, Heilongjiang Bayi Agricultural University, Daqing/P.R.China
Tel: +86-459-15244626625; E-mail: 1431269471@qq.com +
Corresponding author: Chundong WU, Zhanbin GUO
DOI: https://doi.org/10.35633/inmateh-78-109

Keywords: *Anaerobic co-digestion, Long-chain fatty acids, Microbial community, Lipase, PECI enzyme*

ABSTRACT
To elucidate the inhibition mechanisms of sludge-grease anaerobic co-digestion (ACoD) and the microbial community succession patterns, this study systematically investigated the process through an enzyme addition strategy. Results demonstrated that compared with sludge mono-digestion, sludge-grease ACoD significantly enhanced methane yield, with the 1.5% mixed fatty acids group achieving a cumulative methane yield of (666.40±30.71) mL/g VS, representing a 179.4% increase over the control group. An addition of 3% unsaturated long-chain fatty acids (LCFAs) was identified as the inhibitory threshold for anaerobic digestion (AD). Both lipase and PECI (Peroxisomal 3,2-trans-enoyl-CoA isomerase) enzyme addition restored methanogenic activity, with the 1% PECI enzyme treatment group achieving a cumulative methane yield of up to 1627.76 mL/g VS, exhibiting the most effective mitigation. However, the addition of both enzymes showed limited improvement in reducing the lag phase of AD. Microbial community analysis revealed that low concentrations of lipase enriched Synergistetes, thereby facilitating the recovery of methanogenic functions, whereas high concentrations suppressed Synergistetes activity. Low concentrations of PECI enzyme promoted Bacteroidetes to dominate the late-stage degradation, while high concentrations maintained stable Synergistetes metabolic activity, thereby effectively circumventing LCFAs toxicity and acid accumulation risks. These findings provide a theoretical basis and technical reference for the engineering application of AD treating lipid-containing organic wastes.

摘要
为揭示污泥-油脂厌氧共消化的抑制机制及微生物群落演变规律，本研究采用酶添加策略开展系统研究。结果表明，与污泥单独消化相比，污泥-油脂共消化显著提升了甲烷产量，其中 1.5%混合脂肪酸组累积甲烷产量达 (666.40±30.71) mL/g VS，较对照组提高 179.4%。3%不饱和长链脂肪酸被确定为厌氧消化的抑制阈值。添加脂肪水解酶和 PECI (Peroxisomal 3,2-trans-enoyl-CoA isomerase) 酶均可恢复产甲烷活性，其中 1% PECI 酶处理组累积甲烷产量高达 1627.76 mL/g VS，缓解效果最佳，但添加两种酶对厌氧消化滞后期的改善作用有限。微生物群落分析表明：低浓度脂肪水解酶通过富集互营菌门促进产甲烷功能恢复，而高浓度则抑制该菌门活性；低浓度 PECI 酶促进拟杆菌门在后期降解中发挥主导作用，高浓度则通过维持互营菌门代谢稳定性有效规避长链脂肪酸毒性及酸化风险。本研究可为含油脂有机废弃物厌氧消化的工程应用提供理论依据和技术参考。

INTRODUCTION
With rapid industrialization and urbanization, the production of waste-activated sludge (WAS) in Chinese wastewater treatment plants has increased dramatically *(Chen et al., 2022)*. WAS typically contains substantial organic matter and pollutants, and its improper disposal may result in secondary environmental pollution and resource wastage *(Khawer et al., 2022)*. Among various sludge treatment methods, AD has been extensively employed in sludge management owing to its capability to achieve sludge minimization and stabilization while simultaneously promoting energy recovery *(Ferrer et al., 2024)*. However, mono-digestion of sludge presents certain limitations, including low organic matter degradation efficiency, restricted methanogenic performance, and insufficient process stability.

[1]*Chenxi Li, Prof. Ph.D.; Jinku Liu, MS; Mengjie Du, MS; Chundong Wu, Ph.D.; Zhanbin Guo, Prof. Ph.D.;*

In recent years, the ACoD of grease with sludge has garnered substantial research attention. This approach offers distinct advantages. First, grease contains high-energy-density lipids, exhibiting a theoretical methane yield significantly higher than that of sludge alone, thereby substantially enhancing the overall methanogenic performance of the system *(Berninghaus et al., 2022)*. Second, serving as a carbon-rich substrate, grease effectively ameliorates the low C/N ratio typically encountered in sludge mono-digestion, thereby promoting microbial metabolic equilibrium and enhancing AD stability. Third, under optimal mixing ratios, ACoD enhances organic matter degradation efficiency, achieving the dual objectives of synergistic waste valorization and energy recovery *(Astals et al., 2022; Zhang et al., 2014; Tandukar et al., 2022)*.

Despite these advantages, the accumulation of LCFAs—particularly unsaturated fatty acids such as oleic acid (C18:1)—produced from grease hydrolysis under anaerobic conditions exerts significant toxicity toward methanogenic consortia, readily inducing cell membrane damage, metabolic activity inhibition, and reactor operational instability. This issue has emerged as a critical bottleneck hampering the engineering application of this technology. Current mitigation strategies primarily involve physicochemical pretreatment, chemical additives, optimized feeding protocols, or reduced organic loading rates. Nevertheless, these approaches predominantly rely on macroscopic characterization and empirical parameter adjustments, lacking mechanistic insights into LCFAs transformation at the molecular level and corresponding microbial ecological responses. Consequently, control operations often lag behind system destabilization, precluding accurate early warning and proactive intervention.

Based on this, this study addresses the existing research gaps regarding insufficient understanding of unsaturated LCFAs inhibition mechanisms and the lack of diverse regulation strategies, and carries out systematic research: (1) systematically elucidate the influence patterns of LCFAs saturation degree and concentration on organic matter conversion kinetics, methane yield, and system stability during ACoD, thereby determining the inhibitory threshold of unsaturated LCFAs; (2) reveal the mechanistic linkages between unsaturated LCFAs degradation and key functional guilds through analysis of microbial community succession; and (3) on this basis, innovatively introduce a synergistic regulation strategy of lipase enzymes and PECI enzyme, and comparatively evaluate their alleviating effects on high-concentration unsaturated LCFAs inhibition and the underlying microbial ecological mechanisms.

The distinctive feature of this study lies in systematically revealing the action mechanisms of unsaturated LCFAs from a multi-level coupling perspective of "substrate characteristics—microbial response—enzymatic regulation," and proposing a functional enzyme-enhanced regulation pathway, thereby providing novel theoretical underpinning and technical guidance for the optimization of anaerobic digestion processes treating lipid-laden organic wastes.

MATERIALS AND METHODS

Physicochemical Characteristics of Feedstock and Inoculum

The sludge used in this study was collected from the Dongcheng Wastewater Treatment Plant in Daqing City, Heilongjiang Province, China. The inoculum was obtained from a laboratory-scale anaerobic digester operated continuously with cattle manure. Both substrates and inoculum were stored at 4°C before use. The physicochemical characteristics of the feedstock and inoculum are summarized in Table 1. The grease sources selected for the experiments included saturated and unsaturated fatty acids, specifically stearic acid (C18:0) and oleic acid (C18:1), both with purity >95%, purchased from Shanghai Macklin Biochemical Co., Ltd. (Shanghai, China).

Table 1

Physicochemical characteristics of feedstock and inoculum

Raw material	Total solid (TS)	Volatile solid (VS)	Chemical Oxygen Demand (COD)	Total nitrogen (TN)	Ammonia Nitrogen (NH_4+-N)
	[%]	[%]	[g/L]	[g/L]	[g/L]
Sludge	13.08 ± 0.08	7.29 ± 0.11	48.58 ± 0.97	5.82 ± 0.01	4.59 ± 0.01
Inoculum	8.71 ± 0.04	6.62 ± 0.13	44.09 ± 3.03	9.63 ± 0.04	6.17 ± 0.05

Experimental Setup

Batch AD experiments were conducted in 250 mL borosilicate glass serum bottles (Sichuan Shubo Glass Co., Ltd., Sichuan, China) serving as batch anaerobic digesters, as illustrated in Fig. 1. The reactors were equipped with a dual-port silicone septum sealing system.

One port was connected via silicone tubing to a 0.5 L aluminum-plastic composite gas collection bag for biogas collection, while the other port was connected via silicone tubing to a digital pressure gauge (GM522, Zhibiao Instrument Co., Ltd., Zhejiang, China) for real-time monitoring of internal pressure variations and subsequent biogas volume calculation. All connections were verified to ensure complete gas-tightness.

Fig.1 - AD experimental setup

Experimental Design

Effects of LCFAs Saturation Degree and Concentration on AD

Batch experiments were conducted to investigate the characteristics of ACoD of sludge with LCFAs of varying saturation degrees and concentrations. The reactor headspace accounted for 20% of the total volume. The inoculum-to-substrate ratio was set at 2 (on a VS basis) *(Hao et al., 2020)*. A total of 10 experimental groups were established, including one control group (blank control without LCFAs addition), with three replicates for each group. Initially, each reactor was loaded with 62.5 g of sludge and 137.5 g of inoculum. The types and dosages of fatty acids are detailed in Table 2; notably, the mixed group contained C18:0 and C18:1 at a 1:1 volume ratio. The LCFAs' dosages were calculated as the percentage of pure LCFAs volume relative to the working volume, with three concentration levels: 0.5%, 1.0%, and 1.5%, based on the results obtained from preliminary experiments.

Table 2

Types and Concentrations of Fatty Acids

Group	LCFAs type	Dosage [%]
S-1	C18:0	0.5
S-2	C18:0	1.0
S-3	C18:0	1.5
U-1	C18:1	0.5
U-2	C18:1	1.0
U-3	C18:1	1.5
SU-1	C18:1+C18:0	0.5
SU-2	C18:1+C18:0	1.0
SU-3	C18:1+C18:0	1.5
C (Control)	without fatty acids addition	0

After loading substrate and inoculum into the serum bottles according to the specifications in Table 2, the headspace was purged with nitrogen gas for 1 min to remove oxygen, and the bottles were immediately sealed. The reactors were then incubated in a constant-temperature incubator (JDX-211C-GZ, Shanghai Shiping Experimental Equipment Co., Ltd., Shanghai, China) at 37 ± 1 °C. Biogas production and composition were monitored daily during the first 7 days, and subsequently every 2 days. Samples were collected on day 15 (peak methanogenesis phase) and day 35 (declining methanogenic phase), centrifuged at 8000 rpm for 10 min, and the supernatant was aliquoted into 2 mL cryogenic vials and stored at -40 °C for subsequent analysis of LCFAs, VFAs, and microbial communities.

Experiments on Inhibition Alleviation by Different Enzymes

The experimental setup, feedstock sources, and inoculum were as described previously. Based on the results from the previous experiment, the unsaturated LCFAs concentration was set at 3%, with an inoculum-to-substrate ratio of 2.0 (on a VS basis) *(Hao et al., 2020)*. ACoD was performed using 3% C18:1 and activated sludge as substrates to investigate the effects of enzyme addition on the AD process.

Unsaturated LCFAs exert inhibitory effects on AD systems primarily through restricted hydrolysis and blocked β-oxidation processes. Therefore, targeting substrate hydrolysis enhancement and key metabolic step regulation represents an effective approach to alleviating their inhibitory effects. Lipase enzymes can improve lipid hydrolysis efficiency and reduce LCFAs accumulation, whereas PECI enzyme participates in the critical isomerization step during unsaturated fatty acid β-oxidation, thereby promoting their further degradation. Therefore, this study selected lipase enzyme (porcine pancreatic origin, powder form; Shanghai Yuanye Bio-Technology Co., Ltd., Shanghai, China) and PECI enzyme (liquid formulation; ProSpec-Tany TechnoGene Ltd., Ness-Ziona, Israel) to target different limiting steps, thereby achieving targeted regulation of unsaturated LCFAs inhibition.

The concentration of lipase enzyme was expressed as grams of enzyme powder per liter of working volume (kg/L), while PECI enzyme concentration was expressed as milliliters of enzyme liquid per liter of working volume (L/L). A total of seven experimental groups were established, including one control group (without enzyme addition), with three replicates per group. Initially, each reactor was loaded with 62.5 g of sludge and 137.5 g of inoculum, with 3% C18:1 and enzymes added simultaneously. The types and dosages of enzymes are detailed in Table 3, with the dosages determined based on previous preliminary experiments. Following substrate loading according to Table 3, the headspace was purged with nitrogen gas for 1 min to remove oxygen, immediately sealed, and incubated in a constant-temperature incubator (JDX-211C-GZ, Shanghai Shiping Experimental Equipment Co., Ltd., Shanghai, China) at 37 ± 1 °C. Biogas production and composition were monitored every 2 days, using the same gas collection method as described previously. Samples were collected on day 7 (initial response phase) and day 14 (mid-term adaptation phase), centrifuged at 8000 rpm for 10 min, and the supernatant was aliquoted into 2 mL cryogenic vials and stored at -40 °C for subsequent analysis of fatty acids and microbial communities.

Table 3

Types and Concentrations of Enzymes

Group	Enzyme Type	Dosage [%]
A-1	lipase	0.1
A-2	lipase	0.5
A-3	lipase	1.0
B-1	PECI enzyme	0.1
B-2	PECI enzyme	0.5
B-3	PECI enzyme	1.0
C-0	without enzyme addition	0

Analytical Methods and Parameters

Biogas Production methane Analysis

Biogas production was measured using the pressure method. Methane content was analyzed using a gas chromatograph (GC-2014C, Shimadzu Corporation, Kyoto, Japan). The modified Gompertz model was employed to fit the cumulative methane yield data for estimating the kinetic parameters of AD, as shown in Equation (1).

$$G(t) = G_{max} \exp\{-\exp[R_m e/G_{max}(\lambda - t) + 1]\} \quad (1)$$

where, $G(t)$ is the cumulative methane yield at time t (mL/g VS); G_{max} is the maximum methane production potential (mL/g VS); R_m is the maximum methane production rate (mL/(g VS·d)); λ is the lag phase (d); t is the digestion time (d); and e is Euler's number (e = 2.7183).

Physicochemical parameter analysis

TS and VS were determined by the gravimetric method according to GB/T 28731-2012 (Chinese national standard). The pH was measured using a pH meter (PHSJ-4F, Shanghai Leici Product Marketing Center, Shanghai, China). COD, NH_4+-N, and TN were analyzed using a UV-visible intelligent multi-parameter water quality analyzer (LH-3BA(V10), Beijing Lianhua Yongxing Technology Development Co., Ltd., Beijing, China).

Microbial and LCFAs Analysis

Microbial community structure was analyzed by high-throughput sequencing (commercially performed by Shanghai Personal Biotechnology Co., Ltd., Shanghai, China). LCFAs species and concentrations were determined according to GB 5009.168-2016 (Chinese national standard for food safety) using the transesterification method followed by gas chromatography analysis.

Data Analysis

Experimental data are presented as mean ± standard deviation. Data processing was performed using Microsoft Excel 2017, and curve fitting and figure preparation were conducted using OriginPro 2017.

RESULTS and DISCUSSIONS

ACoD Characteristics of Sludge with Different LCFAs

Effects on Cumulative Methane Production

The cumulative methane yields from the ACoD of activated sludge with LCFAs of varying saturation degrees and concentrations are presented in Fig. 2. Compared with the control group, LCFAs addition enhanced methane production rates, exhibiting a distinct dose-response relationship where cumulative methane yield increased with increasing LCFAs concentration. Specifically, the saturated fatty acid group (S group) achieved cumulative methane yields of 420.03 ± 20.57, 525.44 ± 15.58, and 671.16 ± 25.03 mL/g VS at low, medium, and high LCFAs concentrations, respectively, representing increases of 76.1%, 120.2%, and 181.4% relative to the control (238.53 ± 33.48 mL/g VS). The unsaturated fatty acid group (U group) yielded 412.24, 523.44, and 630.16 mL/g VS at corresponding concentrations, with enhancement ratios of 72.6%, 119.4%, and 164.2%, respectively. The mixed fatty acid group (SU group) produced 423.39 ± 24.64, 565.10 ± 30.28, and 666.40 ± 30.71 mL/g VS, surpassing the control by 77.5%, 136.9%, and 179.4%, respectively.

These results indicate that ACoD of activated sludge with LCFAs effectively enhances methanogenesis, with LCFAs concentration serving as a critical factor governing biogas production efficiency. This finding aligns with the observations reported by *Szabo-Corbacho et al. (2024)*. However, the dose-response relationship does not manifest uniformly across all fatty acid types; for instance, the addition of palmitic acid resulted in decreased methane yields at higher concentrations *(Szabo-Corbacho et al., 2024)*. Furthermore, *Yang et al. (2017)* demonstrated that methane production was severely inhibited when LCFAs concentrations exceeded 2.4 g/L, with strong inhibition occurring at 3.6 g/L. Such discrepancies may be attributed to the relatively lower LCFAs loadings employed in the present study or the buffering capacity of the sludge matrix against LCFAs toxicity *(Yang et al., 2017)*.

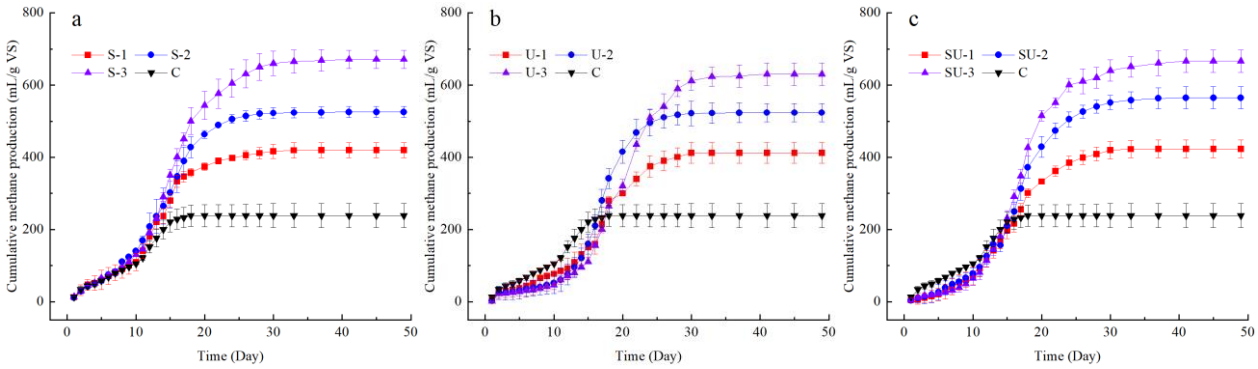

Fig. 2 - Cumulative methane production

a - S group; b - U group; c - SU group

Table 4 presents the kinetic parameters fitted by the modified Gompertz model, including the maximum methane production potential (G_{max}), maximum methane production rate (Rm), and lag phase (λ). The adjusted R^2 values for all treatments exceeded 0.98, indicating excellent model fitting with minimal relative error between predicted and experimental G_{max} values. Compared with the control group, all treatment groups exhibited significantly higher R_m values, likely indicating enhanced methanogenic activity. However, the addition of LCFAs likely markedly prolonged the lag phase (λ), with values of 4.9–5.6 d for the S group, 9.9–10.4 d for the U group, and 6.8–8.2 d for the SU group. Notably, the lag phase of the U group was approximately 1.9-fold that of the S group, indicating that unsaturated fatty acids likely exerted the most pronounced inhibitory effects on the AD process, likely attributable to their higher toxicity *(Dasa et al., 2016)*. The lag phase (λ) reflects the microbial adaptation process to novel substrates, encompassing enzyme system induction, cell membrane repair, and metabolic pathway activation. During this phase, microbial activity remains vulnerable and highly sensitive to environmental stress, rendering the system susceptible to process instability. In the present study, although 1.5% C18:1 did not induce complete process failure, the extension of λ to 10.4 d likely substantially increased operational risks, posing a severe challenge for practical engineering applications.

Table 4

Kinetic parameters fitted by the modified Gompertz model

Substrate	Gmax [mL/g VS]	Rm [mL/g VS·d]	λ [d]	Adjusted R-squared
S-1	433.04 ± 9.18	27.64 ± 1.86	4.88 ± 0.50	0.98
S-2	544.67 ± 9.12	33.93 ± 1.76	5.29 ± 0.39	0.99
S-3	760.41 ± 8.51	49.49 ± 2.36	5.59 ± 0.36	0.99
U-1	420.69 ± 5.69	30.25 ± 1.97	9.88 ± 0.43	0.99
U-2	530.08 ± 7.69	59.31 ± 3.18	10.23 ± 0.23	0.99
U-3	630.02 ± 6.65	38.24 ± 1.25	10.38 ± 0.25	0.99
SU-1	420.12 ± 5.45	29.53 ± 1.25	6.79 ± 0.29	0.99
SU-2	580.12 ± 6.78	38.99 ± 1.84	7.83 ± 0.34	0.99
SU-3	660.29 ± 4.98	54.15 ± 2.27	8.21 ± 0.25	0.99
C	240.13 ± 3.58	16.33 ± 0.93	1.93 ± 0.44	0.98

To identify the inhibitory threshold of unsaturated LCFAs on AD, two additional high-loading treatments, U-4 (2.0% C18:1) and U-5 (3.0% C18:1), were established based on the U-3 treatment (1.5% C18:1). As shown in Fig. 3, cumulative methane production exhibited a significant dose-dependent response to increasing C18:1 concentrations. At the C18:1 concentration of 2.0%, the cumulative methane yield of the U-4 group declined sharply to 302 mL/g VS, representing a significant decrease of 52.1% relative to the U-3 group (630.16 mL/g VS), indicating that methanogenic activity was markedly suppressed. Upon further increasing the concentration to 3.0%, methane generation in the U-5 group ceased almost completely, suggesting that this concentration exceeded the physiological tolerance limit of the methanogenic consortia, resulting in irreversible metabolic inhibition. This threshold phenomenon is likely attributed to the multifaceted toxic mechanisms of LCFAs against anaerobic microorganisms, including: (i) adsorption onto microbial surfaces forming a physical barrier that restricts nutrient access; (ii) disruption of cell membrane integrity leading to the loss of intracellular homeostasis; and (iii) more rapid membrane adsorption kinetics of unsaturated LCFAs compared to their saturated counterparts, thereby exerting stronger toxicity *(Elsamadony et al., 2021; Sun et al., 2025)*. It has also been reported that LCFAs inhibition is theoretically reversible, albeit requiring prolonged recovery periods *(Palatsi et al., 2009)*.

In summary, cumulative methane production exhibited stimulation at low concentrations but inhibition at high concentrations with increasing C18:1 concentration. Following the peak observed in the U-3 group, the U-4 and U-5 groups demonstrated progressive inhibition culminating in complete system failure. These results confirm that the accumulation of high-concentration unsaturated LCFAs represents a critical trigger for process instability in AD systems.

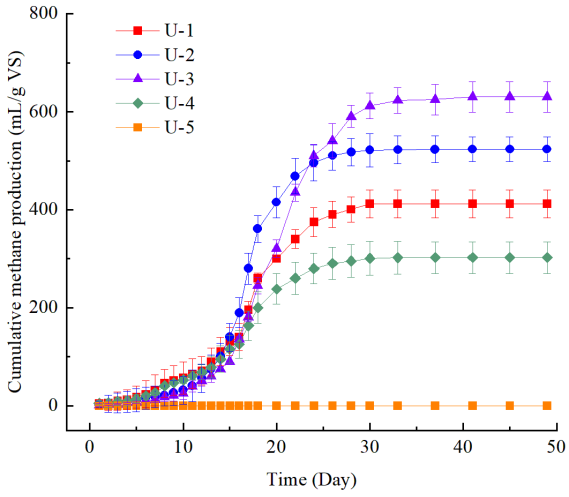

Fig. 3 - Cumulative methane production under varying C18:1 addition levels

Degradation of LCFAs during AD

To elucidate the degradation characteristics of LCFAs with varying saturation degrees during AD, treatments S-1, S-3, U-2, U-3, SU-1, and SU-2 were selected for systematic analysis. As shown in Fig. 4, the LCFAs composition and transformation characteristics differed markedly among treatment groups, reflecting distinct metabolic pathways for saturated versus unsaturated fatty acids.

On day 15 (Fig. 4a), the total LCFAs concentrations in the S-1 and S-3 groups were 313 and 293 μg/mL, respectively, predominantly comprising C16:0 and C18:0 with no detectable C18:1, indicating that saturated fatty acids could readily enter the β-oxidation pathway with efficient metabolic flux. In contrast, the U-2 and U-3 groups exhibited lower total LCFAs levels, while C18:1 persisted with reduced C18:0 content, reflecting limited conversion and inhibitory effects of C18:1 on downstream β-oxidation. The SU-1 and SU-2 groups showed total LCFAs concentrations of 191 and 273 μg/mL, with proportions of C16:0 and C18:0 intermediate between the S and U groups and trace C18:1 residues, suggesting that the mixed addition strategy partially alleviated the inhibitory effects of unsaturated LCFAs and facilitated synergistic degradation.

By day 35 (Fig. 4b), total LCFAs concentrations had declined significantly across all treatments, though degradation efficiencies varied markedly. The S-1 and S-3 groups decreased to 148 and 145 μg/mL, respectively, achieving degradation rates of 52.7% and 50.5%, with the proportion of C16:0 increasing to 65–70%.

This pattern aligns with the characteristic chain-shortening mechanism of classical β-oxidation, wherein C18:0 undergoes sequential β-oxidation cycles to yield C16:0, indicating unobstructed metabolic pathways. In contrast, the U-2 and U-3 groups only decreased to 142 and 150 μg/mL, with degradation rates of merely 1.4% and 21.1%—significantly lower than those observed in the S and SU groups—confirming the persistent inhibition of LCFAs degradation by C18:1. Notably, C18:1 was completely depleted by day 35 in the U groups, having been fully converted to C16:0 and C18:0, a finding that corroborates the classical theory proposed by *Holohan et al. (2022)* that unsaturated LCFAs require initial biohydrogenation to saturated fatty acids before entering the β-oxidation pathway *(Holohan et al., 2022)*. However, this study further reveals that although the hydrogenation step was completed, the toxicity of high-concentration C18:1 toward methanogenic consortia suppressed syntrophic acetate oxidation, preventing the timely consumption of β-oxidation products (acetate and hydrogen). This thermodynamic constraint consequently hindered further degradation *(Usman et al., 2022)*. The SU-1 and SU-2 groups decreased to 142 and 137 μg/mL, with degradation rates of 25.6% and 49.8%, respectively, indicating that the degradation efficiency of the mixed substrate fell intermediate between the S and U groups.

These findings demonstrate that unsaturated fatty acids likely undergo biohydrogenation to saturation before β-oxidation, resulting in substantially compromised overall metabolic efficiency. This "saturation-then-oxidation" transformation pathway explains the molecular mechanisms underlying the prolonged lag phase (approximately 10 d) and suppressed methanogenic activity observed in the U group, while also providing a theoretical basis for subsequent enzyme-enhanced promotion strategies.

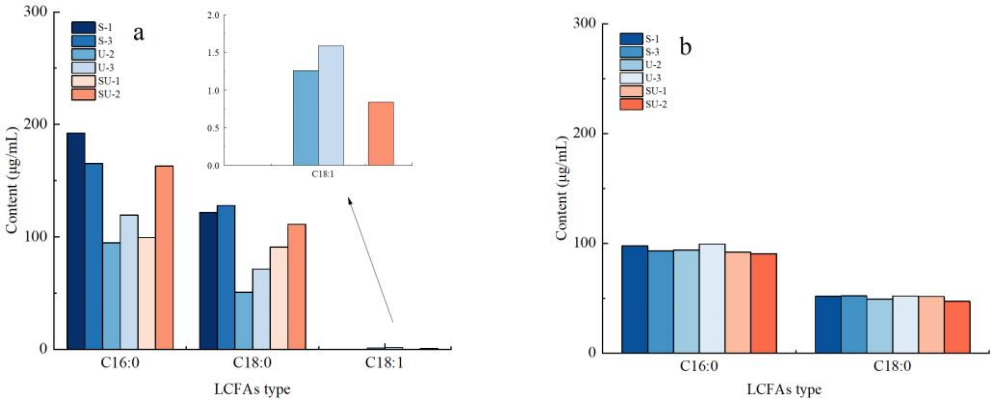

Fig. 4 - Fatty acid composition and transformation

a - Day 15; b - Day 35

During the anaerobic degradation of LCFAs, oleic acid (C18:1) must first undergo biohydrogenation to stearic acid (C18:0) before subsequent β-oxidation to generate volatile fatty acids (VFAs) *(Szabo-Corbacho et al., 2024)*. As shown in Fig. 5, on day 15, the S-1 group exhibited an acetate-dominant profile with acetic acid accounting for 74.99% of total VFAs, indicating a balanced metabolic state. In contrast, the S-3, U-2, U-3, and SU-2 groups displayed significant propionate-type accumulation, with propionic acid representing 81.79%–92.73% of total VFAs. Notably, the U-3 and SU-2 groups showed the highest propionate proportions (84.32% and 92.73%, respectively), which were closely associated with the high residual concentrations of C18:1 and the extended lag phases observed in these treatments. The SU-1 group, with propionic acid comprising 64.82%, demonstrated that the mixed substrate strategy partially alleviated the inhibitory effects of unsaturated fatty acids. By day 35, acetic acid proportions in all treatment groups recovered to 45%–47%, while propionic acid declined to 11%–17%, indicating restoration of metabolic equilibrium.

Propionic acid generated during C18:1 degradation serves not only as a direct inhibitor of methanogenic archaea but also depletes the ecological niche of hydrogenotrophic methanogens, thereby blocking the electron transfer chain required for syntrophic oxidation. Furthermore, high concentrations of unsaturated LCFAs compromise cell membrane integrity and specifically suppresses key hydrolytic guilds such as *Firmicutes*, further exacerbating the propionate metabolic bottleneck *(Usman et al., 2022)*. Consequently, propionate accumulation associated with C18:1 degradation constitutes the core mechanism underlying the significantly extended lag phases and reduced methane yields observed in the U groups.

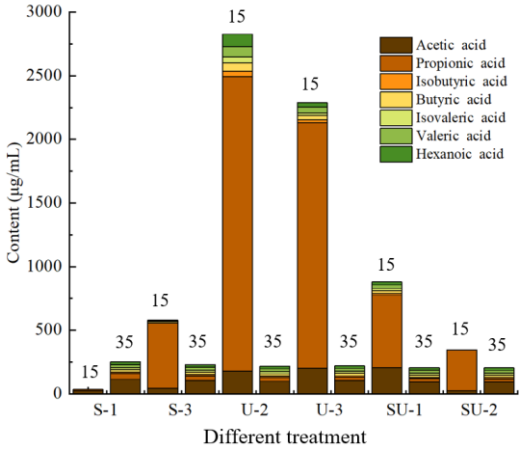

Fig. 5 - Fatty acid distribution on days 15 and 35

Microbial Community Dynamics

Treatments S-2, U-3, and SU-3 were selected to analyze the succession patterns of microbial communities. Fig. 6 presents the phylum-level relative abundance on days 15 and 35. The dominant phyla included *Firmicutes*, *Bacteroidetes*, *Synergistetes*, *Actinobacteria*, and Candidatus *Saccharibacteria*.

As the core hydrolytic-fermentative phylum, *Firmicutes* exhibited a declining trend in abundance throughout the digestion process, with the magnitude of reduction correlating with the LCFAs saturation degree. Specifically, *Firmicutes* decreased from 55% to 50% in the S-2 group (5% reduction), from 54% to 24% in the SU-3 group (30% reduction), and from 73% to 35% in the U-3 group (38% reduction). Previous studies have demonstrated that *Firmicutes* possess superior metabolic capabilities and tolerance toward saturated fatty acids (C18:0), whereas the cytotoxicity of high-concentration unsaturated fatty acids (C18:1) to cell membranes accelerates the loss of ecological niches for this phylum *(Sun et al., 2023)*. This discrepancy suggests that the fatty acid unsaturation degree may serve as a critical factor regulating the community structure of hydrolytic bacteria. As digestion progressed, the abundance of *Bacteroidetes* declined in the S-2 group but increased significantly in the U-3 and SU-3 groups. The concomitant proliferation of *Bacteroidetes* and extended lag phase in the U-3 group indicates that although this phylum can adapt to unsaturated fatty acid environments through adjustments in membrane lipid composition *(Usman et al., 2022)*, its metabolic rate is significantly slower than that of *Firmicutes*, resulting in a "decoupling between bacterial proliferation and methanogenic efficiency" *(Dinova et al., 2023)*. The highest relative abundance of *Synergistetes* was observed in the U-3 treatment, which may be attributed to its metabolic characteristics, utilizing amino acids as primary substrates. Previous studies have indicated that *Synergistetes* are predominantly strictly anaerobic bacteria, with members generally possessing amino acid degradation capabilities and participating in anaerobic organic matter degradation through amino acid fermentation; consequently, they are more likely to gain ecological advantages when amino acid availability increases or when other amino acid-degrading bacteria are inhibited. Meanwhile, Candidatus *Saccharibacteria* typically adopt an epibiotic lifestyle attached to other bacteria and depend on host metabolism for nutrient acquisition. Therefore, in the S-2 and U-3 treatments, Candidatus *Saccharibacteria* exhibited decreasing trends concurrent with the decline in *Actinobacteria* abundance; whereas in the SU-3 treatment, variations in its relative abundance may be associated with changes in host cell metabolic status, thereby affecting the survival conditions of the epibiotic bacteria.

In this study, unsaturated fatty acids appeared to exert selective inhibition on *Firmicutes* while concomitantly promoting the relative enrichment of *Bacteroidetes*. However, given the relatively inferior metabolic efficiency of *Bacteroidetes* in lipid degradation and methanogenic precursor generation, such community shifts may disrupt the synergistic coordination of the hydrolysis-acidogenesis-methanogenesis cascade, thereby extending the system lag phase and compromising methane yields.

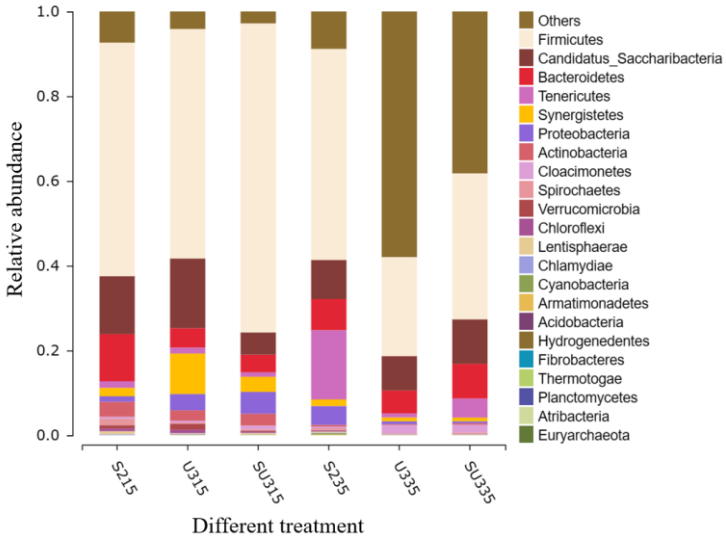

Fig. 6 - Relative abundance of microbial communities at the phylum level on days 15 and 35

Inhibition Alleviation by Different Enzymes

Effects on Methane Production

The addition of an enzyme has been recognized as an effective strategy to alleviate unsaturated fatty acid inhibition and enhance methane production. As shown in Fig. 7, the control group (C-0) receiving 3% C18:1 without enzyme supplementation exhibited complete cessation of methane generation, confirming the pronounced inhibitory effects of high-concentration unsaturated fatty acids on AD. In contrast, supplementation with both lipase enzyme (Fig. 7a) and PECI enzyme (Fig. 7b) restored methanogenic activity, with cumulative methane yields increasing significantly as enzyme dosages increased.

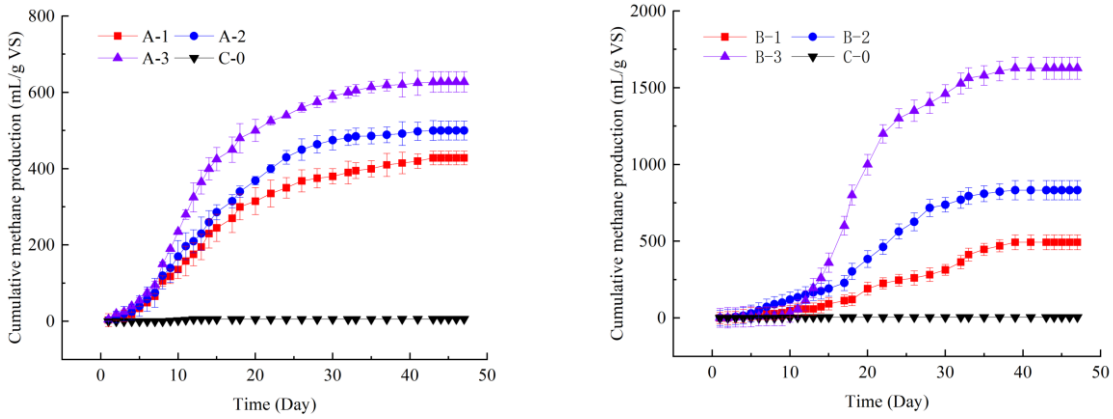

Fig. 7 - Cumulative methane production

a - lipase enzyme addition; b - PECI enzyme addition

In the lipase enzyme group (Group A), cumulative methane yields for treatments A-1, A-2, and A-3 were 428.21, 500.13, and 627.50 mL/g VS, respectively, representing a 46.5% increase in the A-3 group compared with A-1. Lipase enzyme facilitates the hydrolysis of lipid substrates, rendering lipids more accessible to subsequent β-oxidation pathways, thereby improving AD efficiency *(Li et al., 2021)*. However, under high-concentration unsaturated fatty acid conditions, relying solely on lipid hydrolysis may still be subject to LCFAs toxicity, resulting in relatively limited enhancement of methane production. The PECI enzyme group (Group B) demonstrated superior stimulatory effects, with cumulative methane yields of 493.94, 833.13, and 1627.76 mL/g VS for treatments B-1, B-2, and B-3, respectively. The B-3 group exhibited a 229.5% increase compared with B-1, significantly exceeding the enhancement observed in the corresponding lipase enzyme treatments. Compared with the A-3 group (627.50 mL/g VS), the B-3 group (1627.76 mL/g VS) achieved a 159.4% higher methane yield. PECI enzymes function as auxiliary enzymes in β-oxidation, catalyzing the critical isomerization steps during unsaturated fatty acid degradation, thereby facilitating the entry of unsaturated fatty acids into the β-oxidation cycle for subsequent microbial utilization *(Schiaffi et al., 2024)*.

In summary, the results demonstrated that supplementation with both lipase enzyme and PECI enzyme effectively alleviated C18:1-induced inhibition on AD and enhanced methane production, with effects exhibiting a distinct dose-dependent relationship. Notably, PECI enzyme exhibited a stronger stimulatory effect in promoting unsaturated fatty acid degradation, which may be attributed to its direct involvement in the β-oxidation metabolism of unsaturated fatty acids, thereby alleviating the toxic inhibition of LCFAs on methanogenic consortia and significantly improving methane yields.

Table 5 presents the kinetic parameters fitted by the modified Gompertz model. All treatments exhibited excellent model fitting (adjusted $R^2 \geq 0.97$), indicating that the model effectively describes the methane production kinetics in this AD system. As enzyme concentration increased, the maximum methane production rate (Rm) showed an overall upward trend; however, the stimulatory effects of the two enzymes may differed markedly. In the lipase enzyme group (Group A), Rm increased from 17.71 to 31.19 mL/(g VS·d), representing a 76.1% increase. In contrast, the PECI enzyme group (Group B) showed a significant increase in Rm from 17.93 to 127.87 mL/(g VS·d), with an increase of 613.2%. Notably, the Rm of treatment B-3 was approximately 4.1-fold that of A-3, further inferring the higher catalytic efficiency of PECI enzyme in promoting substrate conversion and methane generation.

However, enzyme addition may show limited improvement in reducing the lag phase (λ). The λ in Group A remained within 4.55–5.57 d, whereas Group B exhibited a significantly longer λ of 7.74–9.83 d compared with Group A. This may be attributed to the more efficient hydrolytic activity of the PECI enzyme, leading to a rapid accumulation of LCFAs in the short term and consequently exerting more persistent inhibitory effects on methanogens. In contrast, the lipase enzyme acted more moderately, with a slower release rate of LCFAs, thereby shortening the microbial acclimation period. Notably, the C-0 group (without enzyme addition) showed a relatively shorter λ (8.42 d); however, its extremely low Rm (1.78 mL/(g VS·d)) and $Gmax$ (5.77 mL/g VS) indicated that high-concentration C18:1 may cause severe metabolic inhibition, essentially blocking methane generation. Overall, although enzyme addition inevitably prolonged the λ, it may ultimately achieved significant gains in cumulative methane production by relieving substrate inhibition and enhancing methanogenic activity.

Table 5

Kinetic parameters fitted by the modified Gompertz model

Substrate	Gmax [mL/g VS]	Rm [mL/g VS·d]	λ [d]	Adjusted R-squared
A-1	450.08 ± 4.86	17.71 ± 0.46	4.55 ± 0.27	0.99
A-2	500.13 ± 5.52	19.70 ± 0.50	5.24 ± 0.27	0.99
A-3	627.50 ± 3.03	31.19 ± 0.49	5.57 ± 0.14	0.99
B-1	594.22 ± 22.33	17.93 ± 0.69	9.24 ± 0.51	0.99
B-2	905.48 ± 30.91	36.11 ± 2.62	7.74 ± 0.76	0.97
B-3	1602.89 ± 21.30	127.87 ± 8.25	9.83 ± 0.37	0.99
C-0	5.77 ± 0.05	1.78 ± 0.17	8.42 ± 0.16	0.99

Effects of Enzyme Addition on LCFA Degradation

Figure 8 presents the temporal dynamics of fatty acid composition in AD systems treated with lipase enzyme (Group A) and PECI enzyme (Group B) on days 7 (a) and 14 (b). Collectively, the system was dominated by C16:0, C14:0, and C18:1, with C16:0 constituting the major fraction. Previous studies have demonstrated that lipids are initially hydrolyzed by lipases into LCFAs (e.g., C16:0 and C18:1) during AD, which are subsequently degraded through β-oxidation and ultimately converted to methane *(Shi et al., 2024)*.

On day 7 (Fig. 8a), treatment A-2 exhibited the highest total fatty acid content, with C16:0 constituting the predominant fraction; however, substantial residual C18:1 was also detected. This suggests that although medium-concentration lipase enzyme facilitated lipid hydrolysis, a mismatch between the conversion rate of unsaturated fatty acids and their generation rate resulted in the transient accumulation of LCFAs in the system. In contrast, fatty acid contents in Group B were overall lower than those in Group A, indicating that PECI enzyme could accelerate the conversion of unsaturated fatty acids, enabling C18:1 to enter the β-oxidation pathway more rapidly for microbial utilization. By day 14 (Fig. 8b), treatment A-3 showed a significant increase in total fatty acid content, with C16:0 reaching the highest level, indicating that high-concentration lipase enzyme may have induced rapid lipid hydrolysis, generating substantial quantities of LCFAs that accumulated transiently in the system. Previous studies have demonstrated that LCFAs possess strong adsorption capacity and inhibitory effects in AD systems, and their excessive accumulation exerts adverse effects on methanogenic consortia *(Cirne et al., 2007)*. In contrast, although treatment B-3 still exhibited elevated C16:0 levels, residual C18:1 was markedly reduced, suggesting that PECI enzyme effectively facilitates the conversion of

unsaturated fatty acids to saturated fatty acids for subsequent degradation. Furthermore, treatments B-1 and B-2 showed significantly lower total fatty acid contents compared with other treatments, indicating that optimal PECI enzyme dosage could promote rapid lipid hydrolysis while ensuring prompt microbial utilization of generated LCFAs, thereby mitigating fatty acid accumulation in the system. Overall, the PECI enzyme demonstrated superior efficiency in promoting unsaturated fatty acid conversion and alleviating LCFAs accumulation, thereby facilitating stable operation of the AD system and enhancing methane production.

These results align closely with the kinetic parameters presented in Table 5. Group A exhibited a shorter lag phase (λ) but a lower maximum methane production rate (Rm), reflecting relatively moderate fatty acid release and gradual acclimation of methanogenic consortia. In contrast, Group B showed a longer λ but extremely high Rm, indicating that rapid hydrolysis by PECI enzyme caused an initial LCFAs shock, requiring prolonged microbial acclimation; however, once acclimated, methanogenic efficiency was substantially enhanced. Notably, treatment B-3 achieved an Rm of 127.87 mL/(g VS·d), corresponding to the characteristic of elevated C16:0 accompanied by low C18:1 observed in Fig. 8b, suggesting that lipid hydrolysis and methane generation achieved an optimal balance under these conditions.

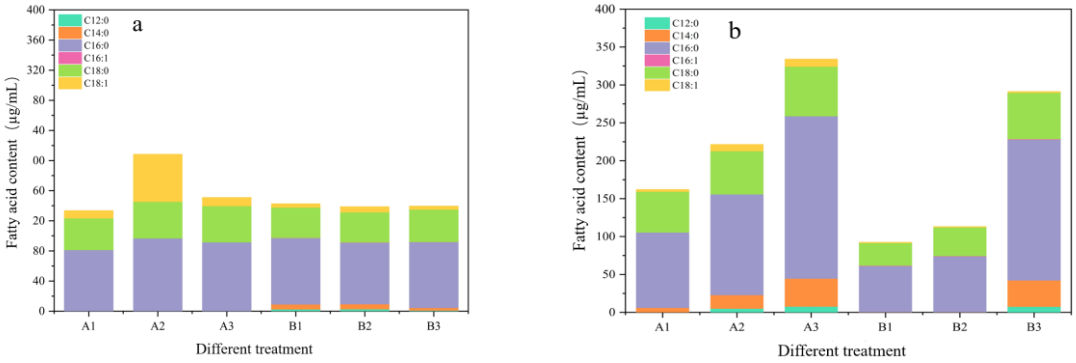

Fig. 8 - Fatty acid composition and transformation

a - Day 7; b - Day 14

Figure 9 presents the composition of VFAs and their temporal dynamics during AD on days 7 (a) and 14 (b). VFAs primarily include acetic acid, propionic acid, butyric acid, isobutyric acid, valeric acid, isovaleric acid, and hexanoic acid, serving as important intermediate metabolites produced during the hydrolysis-acidogenesis stage of AD.

On day 7 (Fig. 9a), treatment A-1 exhibited the highest total VFAs content, with acetic acid accounting for 73%, indicating that low-concentration lipase enzyme primarily promoted lipid hydrolysis and acidogenesis, while methanogenesis had not been fully initiated, resulting in transient accumulation of VFAs. With increasing enzyme concentrations, total VFAs contents in treatments A-2 and A-3 decreased significantly, with acetic acid proportions dropping to 58% and 48%, respectively, indicating that higher-concentration lipase enzyme could accelerate the conversion rate of VFAs to methane, thereby reducing intermediate metabolite accumulation. In contrast, total VFAs contents in Group B were overall lower than those in Group A, with acetic acid proportions maintained between 43% and 54%, indicating that PECI enzyme could more effectively promote substrate hydrolysis and subsequent metabolic processes, enabling the system to maintain better metabolic equilibrium. By day 14 (Fig. 9b), total VFAs contents in all treatments decreased significantly, indicating that VFAs were gradually consumed and entered the methanogenic stage. Specifically, acetic acid proportions in treatments A-1, A-2, and A-3 increased to 60%, 68%, and 72%, respectively, with total VFAs dropping to approximately 300–450 mg/L, indicating that methanogenic activity in the system was gradually enhanced.

Group B demonstrated more pronounced effects, with acetic acid proportions in treatments B-1, B-2, and B-3 reaching approximately 60%, 79%, and 67%, respectively, and contents of propionic acid and other VFAs remaining low, indicating that the PECI enzyme-treated system could more effectively promote the conversion of VFAs to methane.

Overall, Group B maintained consistently lower VFAs accumulation levels throughout the digestion process and exhibited higher acetic acid conversion efficiency, which aligns with the higher methane production rate (R_m) and maximum methane production potential (G_{max}) observed in Table 5. These results indicate that the PECI enzyme can promote the synergistic metabolism of the hydrolysis-acidogenesis-methanogenesis process, thereby alleviating the inhibition by unsaturated fatty acids on the AD system and enhancing methanogenic performance.

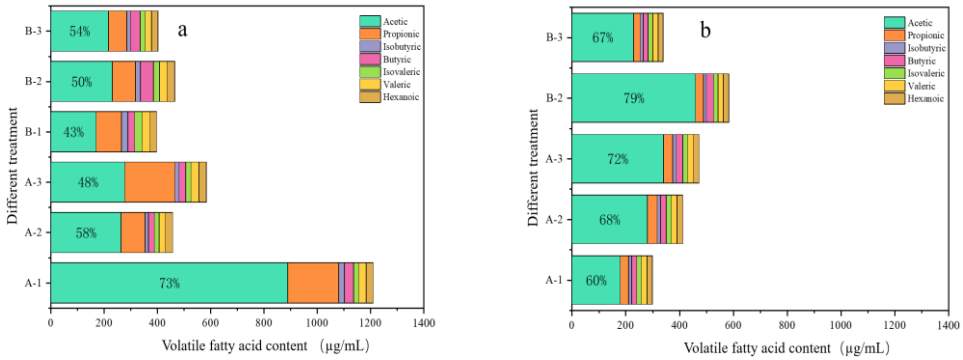

Fig. 9 - VFAs composition and transformation

a - Day 7; b - Day 14

Effects of Enzyme Addition on Microbial Community

Figure 10 presents the succession characteristics of microbial communities at the phylum level in AD systems under enzyme addition conditions. Overall, the dominant phyla included *Firmicutes*, *Bacteroidetes*, *Proteobacteria*, and *Synergistetes*. Among these, *Firmicutes* and *Bacteroidetes* are typically involved in the hydrolysis and acidogenesis of complex organic matter, whereas *Synergistetes* play a key role in the β-oxidation of LCFAs and syntrophic metabolism.

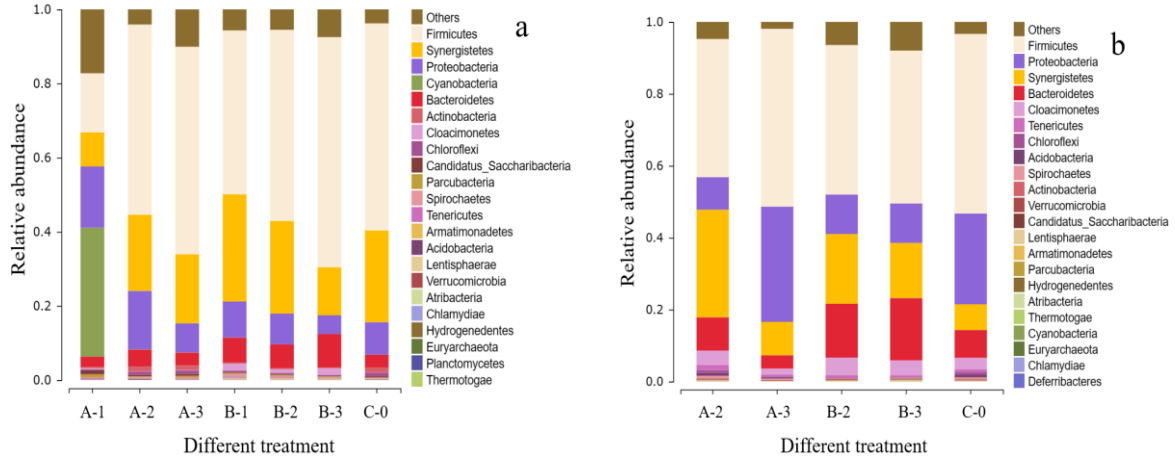

Fig. 10 - Microbial community dynamics

a - Day 7; b - Day 14

From day 7 to day 14, treatment A-2 exhibited decreasing abundances of *Firmicutes* and *Proteobacteria*, whereas *Synergistetes* and *Bacteroidetes* increased in abundance, indicating that system function gradually shifted from initial hydrolysis-acidogenesis toward syntrophic metabolism and methanogenesis as digestion progressed. In contrast, treatment A-3 showed decreasing abundance of *Synergistetes* but significant enrichment of *Proteobacteria*, which may be attributed to the rapid accumulation of LCFAs in the short term caused by high-concentration lipase enzyme, exerting inhibitory effects on *Synergistetes*. Previous studies have demonstrated that LCFAs possess strong toxicity toward anaerobic microorganisms and can suppress the activity of syntrophic β-oxidizing guilds *(Sousa et al., 2009)*, whereas enrichment of *Proteobacteria* is typically associated with system stress response and fatty acid degradation processes. In the PECI enzyme-treated groups, both treatments B-2 and B-3 exhibited relatively stable community structures. Specifically, *Firmicutes* decreased in abundance while *Bacteroidetes* increased, indicating that degradable organic matter gradually decreased following substrate hydrolysis, and the system progressively entered the late-stage metabolic phase. Meanwhile, *Synergistetes* remained relatively stable, suggesting that β-oxidation of LCFAs proceeded continuously, thereby maintaining the synergistic coordination of syntrophic metabolism and methanogenesis. Compared with the lipase enzyme treatment, the PECI enzyme-treated groups overall exhibited more stable community structure and higher syntrophic metabolic potential, which aligns with their higher methane production rates and lower VFAs accumulation.

Overall, the two enzymes regulated microbial community structure in AD through distinct mechanisms. Lipase enzyme at low concentrations facilitated the enrichment of functional guilds such as *Synergistetes*; however, high concentrations could lead to LCFAs accumulation and suppress key *Synergistetes*.

In contrast, PECI enzyme maintained a stable abundance of *Synergistetes* and promoted *Bacteroidetes* participation in late-stage organic matter degradation, thereby establishing a more stable hydrolysis-acidogenesis-methanogenesis metabolic network and enhancing anaerobic digestion efficiency.

This study obtained microbial community relative abundance information based on high-throughput sequencing technology, and the conclusions are based solely on relative abundance. Changes in community structure do not necessarily reflect actual microbial activity or functional changes; therefore, the relevant results should be interpreted in conjunction with functional indicators.

CONCLUSIONS

This study systematically elucidated the inhibition mechanisms of C18:1 on sludge ACoD and enzyme-enhanced mitigation strategies from the perspectives of molecular transformation mechanisms of unsaturated LCFAs and microbial community interactions. The principal novel findings include: (1) establishing 3% C18:1 as the functional inhibitory threshold for AD, revealing that its "biohydrogenation-to-saturation before β-oxidation" transformation pathway results in compromised metabolic efficiency, thereby supplementing current understanding of the differentiated metabolic behaviors between unsaturated and saturated LCFAs; (2) elucidating the ecological mechanism by which C18:1 selectively suppresses Firmicutes while promoting inefficient proliferation of Bacteroidetes, thereby disrupting functional coupling within the hydrolysis-acidogenesis-methanogenesis metabolic chain from the perspective of microbial cooperation; and (3) establishing a concentration-dependent enzymatic regulation strategy, demonstrating that PECI enzyme exhibits superior capacity compared to lipase enzyme in maintaining stable Synergistetes activity and constructing an efficient metabolic chain. These findings provide a theoretical basis for enzymatic optimization in the anaerobic digestion of grease-containing organic wastes; however, the applicability of batch experimental results to continuous-flow operational conditions requires further validation.

ACKNOWLEDGEMENT

This study was financially supported by the annual innovation research plan of Daqing Petroleum Management Bureau Co., Ltd. (Daqing, China) (No. dqc-2021-qt-ky-001), Heilongjiang Bayi Agricultural University Natural Science Talent Support Plan (No. ZRCQC202005), Heilongjiang Bayi Agricultural University Talent Research Initiation Plan (No. XYB202001) and Heilongjiang Bayi Agricultural University Natural Science Talent Support Program (No. ZRCPY202206).

REFERENCES

[1] Astals, S., Batstone, D. J., Mata-Alvarez, J., & Jensen, P. D. (2014). Identification of synergistic impacts during anaerobic co-digestion of organic wastes. *Bioresource technology*, vol. 169, pp. 421-427.

[2] Berninghaus, A. E., & Radniecki, T. S. (2022). Shock loads change the resistance, resiliency, and productivity of anaerobic co-digestion of municipal sludge and fats, oils, and greases. *Journal of Cleaner Production*, vol. *362*, pp. 132447.

[3] Cirne, D. G., Paloumet, X., Björnsson, L., Alves, M. M., & Mattiasson, B. (2007). Anaerobic digestion of lipid-rich waste—Effects of lipid concentration. *Renewable energy*, vol. 32, no. 6, pp. 965-975.

[4] Chen, W., Liu, J., Zhu, B. H., Shi, M. Y., Zhao, S. Q., He, M. Z., ... & Chen, Y. P. (2022). The GHG mitigation opportunity of sludge management in China. *Environmental research*, vol. 212, pp. 113284.

[5] Dasa, K. T., Westman, S. Y., Millati, R., Cahyanto, M. N., Taherzadeh, M. J., & Niklasson, C. (2016). Inhibitory Effect of Long-Chain Fatty Acids on Biogas Production and the Protective Effect of Membrane Bioreactor. *BioMed Research International*, vol. 2016, no.1, pp. 7263974.

[6] Dinova, N., Peng, W., Kirilova-Belouhova, M., Li, C., Schneider, I., Nie, E., ... & He, P. (2023). Functional and molecular approaches for studying and controlling microbial communities in anaerobic digestion of organic waste: a review. *Reviews in Environmental Science and Bio/Technology*, vol. 22, no. 3, pp. 563-590.

[7] Elsamadony, M., Mostafa, A., Fujii, M., Tawfik, A., & Pant, D. (2021). Advances towards understanding long chain fatty acids-induced inhibition and overcoming strategies for efficient anaerobic digestion process. *Water Research*, vol. 190, pp. 116732

[8] Ferrer, I., Passos, F., Romero, E., Vázquez, F., & Font, X. (2024). Optimising sewage sludge anaerobic digestion for resource recovery in wastewater treatment plants. *Renewable Energy*, vol. 224, pp. 120123.

[9] Hao, J., & He, X. (2020). Fat, oil, and grease (FOG) deposits yield higher methane than FOG in anaerobic co-digestion with waste activated sludge. *Journal of environmental management*, vol. 268, pp. 110708.
[10] Holohan, B. C., Duarte, M. S., Szabo-Corbacho, M. A., Cavaleiro, A. J., Salvador, A. F., Pereira, M. A., ... & Alves, M. M. (2022). Principles, advances, and perspectives of anaerobic digestion of lipids. *Environmental science & technology*, vol. 56, no. 8, pp. 4749-4775.
[11] Khawer, M. U. B., Naqvi, S. R., Ali, I., Arshad, M., Juchelková, D., Anjum, M. W., & Naqvi, M. (2022). Anaerobic digestion of sewage sludge for biogas & biohydrogen production: State-of-the-art trends and prospects. *Fuel*, vol. 329, pp. 125416.
[12] Li, X., & Shimizu, N. (2021). Effects of lipase addition, hydrothermal processing, their combination, and co-digestion with crude glycerol on food waste anaerobic digestion. *Fermentation*, vol. 7, no. 4, pp. 284.
[13] Palatsi, J., Laureni, M., Andrés, M. V., Flotats, X., Nielsen, H. B., & Angelidaki, I. (2009). Strategies for recovering inhibition caused by long chain fatty acids on anaerobic thermophilic biogas reactors. *Bioresource technology*, vol. 100, no. 20, pp. 4588-4596.
[14] Sousa, D. Z., Smidt, H., Alves, M. M., & Stams, A. J. (2009). Ecophysiology of syntrophic communities that degrade saturated and unsaturated long-chain fatty acids. *FEMS microbiology ecology*, vol. 68, no. 3, pp .257-272.
[15] Sun, M., Zhang, C., Shi, Z., Zhang, C., Zhang, S., & Luo, G. (2023). Genome-centric metagenomic analysis revealed the microbial shifts in response to long-chain fatty acids (LCFA) in anaerobic digestion with hydrochar. *Chemical Engineering Journal*, vol. 466, pp. 143249.
[16] Schiaffi, V., Barras, F., & Bouveret, E. (2024). Matching the β-oxidation gene repertoire with the wide diversity of fatty acids. *Current Opinion in Microbiology*, vol. 77, pp. 102402.
[17] Shi, E., Zou, Y., Zheng, Y., Zhang, M., Liu, S., Zhang, S., & Zhang, X. (2024). Kinetic study on anaerobic digestion of long-chain fatty acid enhanced by activated carbon adsorption and direct interspecies electron transfer. *Bioresource Technology*, vol. 403, pp. 130902.
[18] Sun, M., Cheng, Y., Jiang, T., Zhang, Y., Zhang, S., & Luo, G. (2025). Hydrochar relieved long chain fatty acids (LCFA) inhibition in continuous anaerobic reactor treating food waste. *Bioresource Technology*, vol. 432, pp. 132658.
[19] Tandukar, M., & Pavlostathis, S. G. (2022). Anaerobic co-digestion of municipal sludge with fat-oil-grease (FOG) enhances the destruction of sludge solids. *Chemosphere*, vol. *292*, pp. 133530.
[20] Usman, M., Zhao, S., Jeon, B. H., Salama, E. S., & Li, X. (2022). Microbial β-oxidation of synthetic long-chain fatty acids to improve lipid biomethanation. *Water research*, vol. 213, pp. 118164.
[21] Yang, Z., Wang, W., Ma, Z., Chen, H., & Liu, G. (2017). Effects of long-chain fatty acids on methane production from food waste anaerobic digestion(长链脂肪酸对餐厨垃圾厌氧消化产甲烷的影响), *Chinese Journal of Environmental Engineering*, vol. 11, no. 10, pp. 5651–5657.
[22] Zhang, C., Su, H., Baeyens, J., & Tan, T. (2014). Reviewing the anaerobic digestion of food waste for biogas production. *Renewable and Sustainable Energy Reviews*, vol. 38, pp. 383-392.